Incoherent holographic imaging through thin turbulent media

Natan T. Shaked [a,*], Yitzhak Yitzhaky [b], Joseph Rosen [a]

[a] Department of Electrical and Computer Engineering, Ben-Gurion University of the Negev, P.O. Box 653, Beer-Sheva 84105, Israel
[b] Department of Electro-Optics Engineering, Ben-Gurion University of the Negev, P.O. Box 653, Beer-Sheva 84105, Israel

ABSTRACT

We introduce and experimentally demonstrate a new method of computing Fresnel holograms of a real-existing, three-dimensional (3-D) scene hidden behind a thin turbulent medium, and illuminated by incoherent white light. From each perspective point of view, we acquire multiple noisy speckled images through the medium vibrated mechanically. These images are fused together to yield a smoothed perspective projection of the hidden 3-D scene. All smoothed projections are processed to yield a Fresnel hologram of the hidden scene. The 3-D image reconstructed from the hologram is further improved by digital blind deconvolution of each of the 3-D image slices with its own estimated impulse response.

© 2009 Elsevier B.V. All rights reserved.

1. Introduction

Three-dimensional (3-D) optical imaging of objects embedded in scattering media has gained an increased attention in the recent years due to its vast number of practical applications. Medical optical imaging for diagnostic purposes is one of these applications. It has the advantages of being non-ionizing, safe, and inexpensive compared to the widely-used X-ray computed tomography (CT). Various optical coherence tomography and spectroscopic techniques [1,2] have been proposed in the literature as alternatives to CT. However, most of these methods require the use of partially-incoherent light sources and interferometric optical setups, imposing practical limitations on the systems. Other studies showed that a dynamic analysis of modulated optical speckled patterns of biological tissues can be obtained by ultrasound vibration [3,4].

Several years ago, our group demonstrated two-dimensional (2-D) imaging of objects embedded in biological tissues [5]. In this technique, called noninvasive optical imaging by speckle ensemble (NOISE), the biological tissues are illuminated by a laser and observed from multiple viewpoints by a microlens array. The multiple viewpoint images are centered and summed together to yield a 2-D image of the embedded objects. Stereoscopic version of the NOISE technique is able to obtain 3-D stereoscopic imaging of the embedded objects [6]. Recently, a coherent non-holographic integral imaging method of 3-D objects embedded in a scattering medium has been presented by Moon and Javidi [7].

Holography, however, has several advantages compared to other 3-D imaging methods. Holography provides the most authentic 3-D illusion to the human eye, with accurate depth cues, and without the need for special viewing devices. In addition, 3-D information can be stored in a very dense and encrypted way by holograms. Yu and Kim have presented a topographic imaging method that is based on wavelength-scanning digital interference holography using a dye laser [8].

In the current paper, we suggest a new method for 3-D holographic imaging of real-existing objects that are hidden behind a turbulent medium. In the proposed system, we use spatially and temporary incoherent illumination, and any special light sources, interferometric optical setups, or lasers of any kind are not required. In fact, since the proposed holograms are generated digitally under incoherent illumination, most of the disadvantages characterizing conventional holographic recording, namely, the need for a coherent, powerful laser source and an extreme stability of the optical system as well as long developing process of the recorded hologram, are avoided.

The proposed method is inspired by the NOISE technique. However, this time we view the scene from different perspectives to get holographic imaging of the 3-D scene, rather than simple 2-D imaging. In addition, the capturing process is performed under incoherent white-light illumination, rather than using laser light as was performed by the NOISE technique.

Shacham et al. [9] have lately suggested a technique for restoring 2-D images of objects viewed through the atmosphere by blindly detecting the best step-edge of the distorted image, estimating the impulse response of the diffusing system, and deconvolving the image with the estimated impulse response to yield an improved image. The current paper also shows how to adapt

* Corresponding author.
E-mail address: natis@ee.bgu.ac.il (N.T. Shaked).

this image restoration method to holography of 3-D objects and to further improve the 3-D image reconstructed from the hologram.

2. Description of the method

Fig. 1 illustrates the proposed optical system. As seen in this figure, the turbulent medium that hides the 3-D scene is illuminated by an incoherent white-light source and vibrated mechanically. For each perspective point of view, many speckled images are acquired through the medium and summed into a single and a relatively-clear perspective projection of the hidden 3-D scene. The reason for that is because the summation process of many random noisy images of the same deterministic hidden signal averages out the noise and consequently exposes the hidden signal. This process is repeated for many perspective points of view located on a transverse plane relative to the 3-D scene. Next, each smoothed projection is multiplied by the same quadratic phase function and the result is summed and introduced into the corresponding pixel in the modified Fresnel hologram [10] of the hidden 3-D scene.

For simplicity, let us assume 1:1 magnification through the entire optical system. The original diffraction-limited projection $P^0_{m,n}(x,y)$ of the 3-D scene, acquired from the (m,n)th point of view without the presence of the turbulent medium, is defined as follows:

$$P^0_{m,n}(x,y) = I_{m,n}(x,y) * |h^0_{m,n}(x,y)|^2, \tag{1}$$

where $I_{m,n}(x,y)$ is the intensity of the object observed from the (m,n)th point of view, $*$ denotes 2-D convolution, and $|h^0_{m,n}(x,y)|^2$ is the intensity impulse response (IIR) [11] of the incoherent optical system from the (m,n)th point of view, without the presence of the turbulent medium. Similarly, the kth speckled projection $P^k_{m,n}(x,y)$ of the 3-D scene, acquired through the vibrated turbulent medium from the (m,n)th point of view, is given by

$$P^k_{m,n}(x,y) = I_{m,n}(x,y) * |h^k_{m,n}(x,y)|^2, \tag{2}$$

where $|h^k_{m,n}(x,y)|^2$ is the IIR of the system, when the hidden 3-D scene is observed from the (m,n)th point of view through the turbulent medium frozen at its kth position.

Under the assumption that the turbulent medium satisfies the statistics of Rytov model with weak phase modulation or Born model [12], it is claimed that

$$(1/K) \cdot \sum_{k=1}^{K} h^k_{m,n}(x,y) \cong \gamma h^0_{m,n}(x,y), \tag{3}$$

where K is a large number of speckled projections taken from each perspective projection during the temporal change in the vibrating

medium, and γ is a constant satisfying $0 < |\gamma| < 1$. The assumption given by Eq. (3) is well satisfied for a phase screen of the form $H^k_{m,n}(f_x,f_y) = H^0_{m,n}(f_x,f_y)\exp[i\Delta\varphi^k_{m,n}(f_x,f_y)]$, where $H^0_{m,n}(f_x,f_y)$ and $H^k_{m,n}(f_x,f_y)$ are the 2-D Fourier transforms of $h^0_{m,n}(x,y)$ and $h^k_{m,n}(x,y)$, respectively, and $\Delta\varphi^k_{m,n}(f_x,f_y)$ is a random phase shift satisfying the following:

$$(1/K) \cdot \sum_{k=1}^{K} \exp[i\Delta\varphi_k(f_x,f_y)] \cong \gamma. \tag{4}$$

This description is typical for a diffuser with statistically invariant phase perturbations all over its area which moves from kth to $(k+1)$th position a much larger distance than the typical perturbation size, such as the diffuser used in the experiment described in Section 3. From Eq. (3), it can be shown that

$$(1/K) \cdot \sum_{k=1}^{K} |h^k_{m,n}(x,y)|^2 \cong (2\gamma - 1)|h^0_{m,n}(x,y)|^2 + \sigma^2_{m,n}(x,y) \equiv \xi(x,y), \tag{5}$$

where $\sigma^2_{m,n}(x,y) = (1/K) \cdot \sum_{k=1}^{K} |h^k_{m,n}(x,y) - h^0_{m,n}(x,y)|^2$ is the variance of the random set $\{h^k_{m,n}(x,y)\}$, and $\xi(x,y)$ is defined to shortly represent the middle expressions in Eq. (5). Using Eqs. (2) and (5), the average speckled projection $\overline{P}_{m,n}(x,y)$ of the hidden 3-D scene, acquired through the vibrated medium from the (m,n)th point of view, is given by

$$\begin{aligned}
\overline{P}_{m,n}(x,y) &= (1/K) \cdot \sum_{k=1}^{K} P^k_{m,n}(x,y) \\
&= (1/K) \cdot \sum_{k=1}^{K} I(x,y) * |h^k_{m,n}(x,y)|^2 \\
&\cong (2\gamma - 1)I(x,y) * |h^0_{m,n}(x,y)|^2 + I(x,y) * \sigma^2_{m,n}(x,y).
\end{aligned} \tag{6}$$

The first term in the last part of Eq. (6) is the (m,n)th original projection $P^0_{m,n}(x,y)$ of the 3-D scene acquired without the presence of the turbulent medium, as given by Eq. (1), multiplied by a constant. The second term in the last part of Eq. (6) is the convolution between the scene intensity from the (m,n)th point of view and the variance function of the set $\{h^k_{m,n}(x,y)\}, k = 1, \ldots, K$. Due to the fact that the turbulent medium broadens the original projection of a point at the scene, $\sigma^2_{m,n}(x,y)$ is wider than $|h^0(x,y)|^2$ and thus the original projection is blurred in accordance with the variance size. However, as we demonstrate in the following, the averaging technique improves dramatically the imaging through the turbulent media as long as the minimum resolvable image size Δ is wider than the diameter of a cylinder which has the same maximum height and total volume of the average IIR. This condition is expressed by
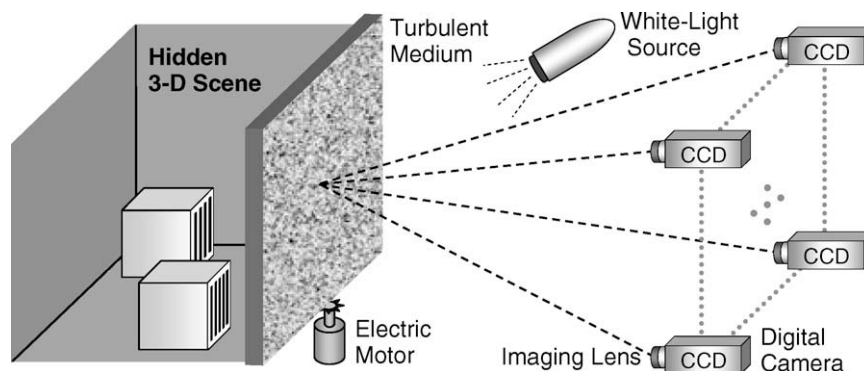

Fig. 1. Optical system for acquiring perspective projections of a 3-D scene hidden behind a turbulent medium, for generating a Fresnel hologram of the hidden scene under incoherent light.

$$\varepsilon \equiv 2\sqrt{\frac{\int\int \xi(x,y)\mathrm{d}x\mathrm{d}y}{\pi\xi(0,0)}} < \Delta. \qquad (7)$$

The practical intuitive meaning of this description is that if the diffuser moves fast enough, one should be able to see through it details of the hidden scene that he could not see through the static diffuser.

Based on the set of the average speckled projections, a modified Fresnel hologram [10] of the 3-D scene is generated by multiplying the (m,n)th average projection by the same quadratic phase function, used for all of the average projections, and summing up the result into the (m,n)th pixel in the hologram complex matrix F, according to the following formula:

$$F(m,n) = \int\int \overline{P}_{m,n}(x,y)\exp[i2\pi b(x^2 + y^2)]\mathrm{d}x\mathrm{d}y, \qquad (8)$$

where b is an adjustable parameter. We have shown in Ref. [10] that in case of using the original projection $P_{m,n}^0(x,y)$, instead of the average projection $\overline{P}_{m,n}(x,y)$, Eq. (8) represents a modified Fresnel hologram of the 3-D scene. For many turbulent media, the condition in Eq. (7) is satisfied, so that $\overline{P}_{m,n}(x,y)$ is a good approximation of $P_{m,n}^0(x,y)$, and thus has an improved resolving power compared with any $P_{m,n}^k(x,y)$. Hence, $F(m,n)$ is a good approximation of the modified Fresnel hologram of the 3-D scene hidden behind the vibrated turbulent medium. Note that the hologram is generated under regular white-light illumination, where no interference is involved in the process. In spite of this, under the assumption that the hidden 3-D scene itself is opaque, the resulting hologram (given as digital complex 2-D matrix) is, in essence, equivalent to the complex amplitude distribution of an optical Fresnel hologram (without adding a reference beam) of this scene recorded from the central point of view. Further details about the modified Fresnel hologram generation process, including the mathematical validation of the abovementioned equivalence, can be found in Ref. [10].

The 3-D image can be digitally reconstructed by a convolution of the hologram with a quadratic phase function, scaled according to the reconstruction distance, as follows:

$$s(m,n;z_r) = F(m,n) * \exp[-i2\pi(m^2 + n^2)/(\beta z_r)], \qquad (9)$$

where β is a constant, and $s(m,n;z_r)$ is the reconstructed 3-D image slice (plane) located at axial distance z_r from the hologram.

To improve the reconstructed 3-D image, we implement a digital blind restoration method that can find the best (closest to ideal) step-edge in each reconstructed plane of the 3-D image without any prior knowledge of the hidden 3-D scene. The only assumptions required are: (a) the blur, which occurs due to the transition of the image through the entire optical system, has isotropic statistical properties; and (b) the image transition is a linear space-invariant degradation process. Based on these assumptions, the improved reconstructed plane can be found by using the five-step algorithm illustrated in Fig. 2. This algorithm is applied to each reconstructed plane separately, while improving the entire 3-D image. A unique advantage of this algorithm for digital holography is that it improves the images of focused objects in each reconstructed plane more than the images of the unfocused objects (the ones which are not located at the proper axial distance in the real 3-D scene).

In its first stage, the algorithm performs edge detection in each reconstructed plane by using the Canny edge detector (since this edge detector produces a single-line edge with a width of one pixel [13]). In the next stage, the algorithm locates the long straight edges in two phases. Firstly, these properties are evaluated for small (3×3 pixel) regions around each pixel, and secondly, the evaluation is extended for larger edge lengths [9]. The best long and straight edges pass to the next algorithm stage, in which the step-edge with the highest contrast and homogeneous regions from both sides is chosen by looking for the step-edge with the highest value of $E\{(x - \mu)^2\}^3/E\{(x - \mu)^4\}$, where μ is the mean of the values x in the square region, and $E\{\cdot\}$ represents the expected value operation [9].

In the next algorithm stage, the chosen step-edge is rectified (if it is not rectified already) to form a vertical (or horizontal) approximation of the step-edge, which is more convenient for further digital processing. Then, the derivative of the monotonic-gradient area in the step-edge is calculated (disregarding the area beyond it). Following the theorem that the derivative of the step response function is equal to the impulse response function, and assuming isotropic blurring statistics, the derivative of the step-edge (selected at any direction) would be a good approximation of the impulse response $t(m,n;z_r)$ of the system. Finally, the improved reconstructed plane $\hat{s}(m,n;z_r)$ is obtained by Wiener filtering:

$$\hat{s}(m,n;z_r) = \mathfrak{F}^{-1}\left\{\frac{\mathfrak{F}\{s(m,n;z_r)\}}{\mathfrak{F}\{t(m,n;z_r)\}} \cdot \frac{|\mathfrak{F}\{t(m,n;z_r)\}|^2}{|\mathfrak{F}\{t(m,n;z_r)\}|^2 + \eta}\right\}, \qquad (10)$$

where $\mathfrak{F}$ and $\mathfrak{F}^{-1}$ denotes 2-D Fourier transform and inverse Fourier transform, respectively, and η is an adjustable constant inversely proportional to the signal to noise ratio [9].

3. Experimental results

We have implemented the optical system shown in Fig. 1, but for simplicity we acquired the projections only along the transverse horizontal axis and generated the hologram on a single axis, instead of acquiring the projections on a 2-D transverse grid and generating the hologram on two axes. Note that, as we have shown in Refs. [14,15], other projection acquisition methods are possible, including using microlens, macrolens, or camera arrays. These methods are faster and they enable the acquisition of dynamic scenes.

A plastic diffuser was used as the turbulent medium and the temporal changes in the medium were implemented by rotating it at the rate of 7000 RPM and vibrating it at a low frequency using an electric motor. The diffuser contained random pattern of plastic bubbles with average size of 2.5 mm and thickness of 0.3 mm. The distance between the digital camera and the diffuser was 55 cm. The 3-D scene hidden behind the diffuser contained two 5 cm × 5 cm cubes positioned at different transverse and axial locations. The first cube contained five bold vertical strips and was located 4 cm behind the diffuser, whereas the second cube contained four bold vertical strips and was located 7 cm to the right of the first cube and 6 cm behind the diffuser. The digital camera was shifted horizontally across a range of 25 cm, and 1100 perspective projections were acquired. A point source of
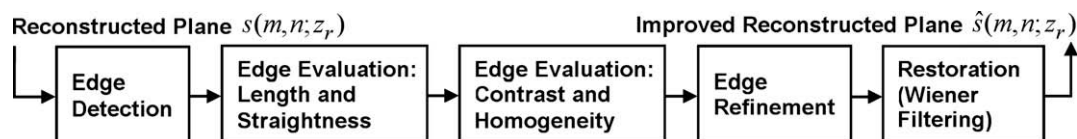

Fig. 2. Automatic algorithm for further improvement of the 3-D image reconstructed from the hologram.

light with diameter of 0.3 mm, located behind the diffuser at the axial distance of the far cube, yielded an IIR diameter of $\varepsilon = 5.17$ pixels, which is smaller than the smallest detail size of the imaged strip patterns ($\Delta = 12$ pixels in our case), and thus we satisfy Eq. (7).

For comparison purposes, three different sets of projections were acquired. The first set, the middle projection of which is shown in Fig. 3a, was acquired without the presence of the diffuser (capturing the 3-D scene directly); The second set, the middle projection of which is shown in Fig. 3b, was acquired through a stationary diffuser (without activating the electric motor); The third set, the middle projection of which is shown in Fig. 3c, was acquired through the rotated/vibrated diffuser, where the averaging of the projections, mentioned in Eq. (6), was obtained by increasing the imaging integration time of the digital camera to 0.1 second, so that the number of summed images for each projection snapshot was $K = 100$. Based on these three sets of projections, three modified Fresnel holograms were generated by multiplying each projection in each set by the same quadratic phase function and summing the result, according to Eq. (8), into the corresponding pixel in the suitable hologram. The magnitude and phase of these holograms are shown in Fig. 4a–c. Each one of these three holograms was reconstructed digitally by using Eq. (9). Since a modified Fresnel hologram has a constant magnification regardless of the axial position [10], the reconstructed planes obtained from each hologram have been rescaled along the horizontal axis according to the reconstruction axial distance, so that the aspect ratios of the original objects have been retained. Fig. 5a and b show the rescaled best-in-focus reconstructed planes obtained from the hologram of the 3-D scene without the presence of the diffuser. As can be seen from these figures, at each of the planes only one cube
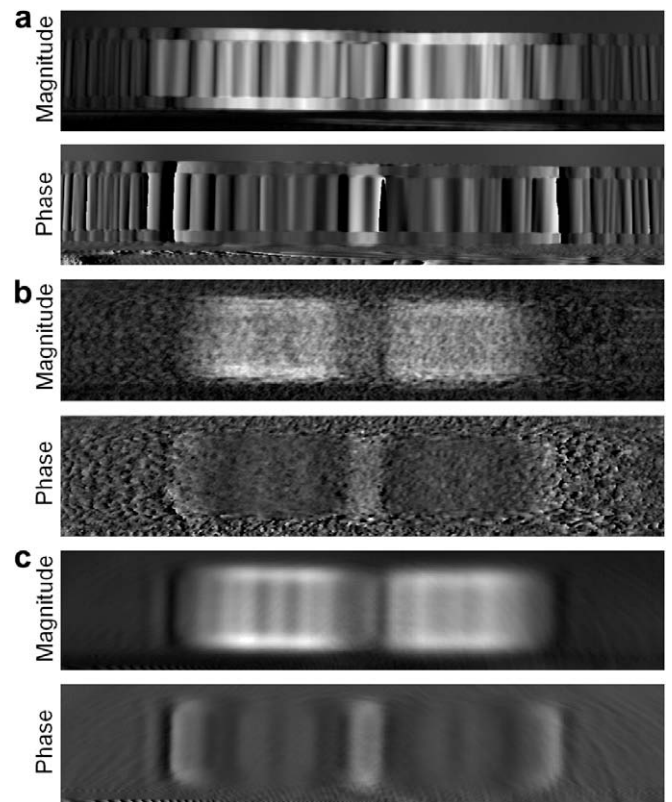

Fig. 4. Magnitudes and phases of the holograms that were generated: (a) without a diffuser; (b) through a stationary diffuser; (c) through a rotated/vibrated diffuser.
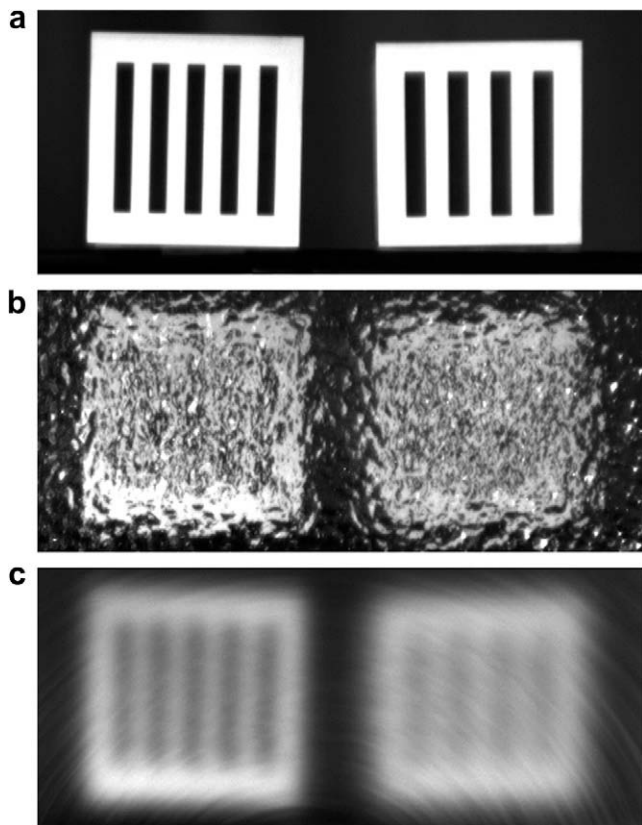

Fig. 3. The middle perspective projection (out of the set of 1100 perspective projections) of the 3-D scene directly acquired by the digital camera: (a) without a diffuser; (b) through a stationary diffuser; (c) through a rotated/vibrated diffuser.
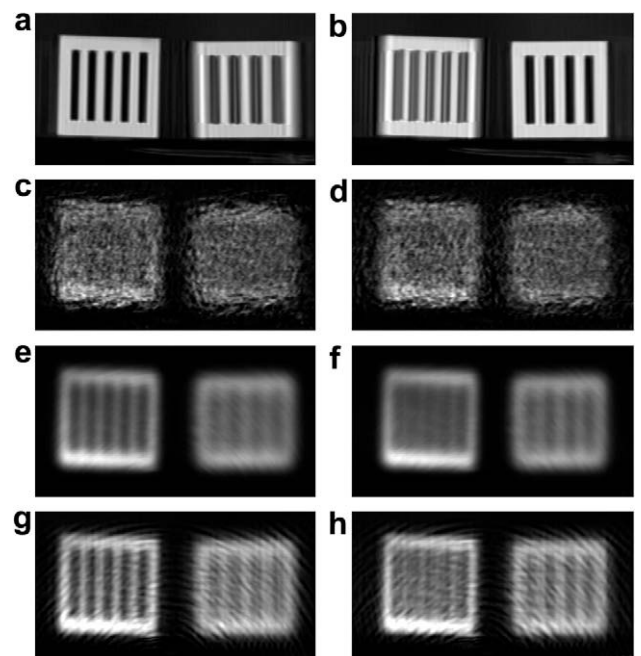

Fig. 5. Best-in-focus reconstructed planes obtained from the holograms that were generated: (a, b) without a diffuser; (c, d) through a stationary diffuser; (e, f) through a rotated/vibrated diffuser; (g, h) after blind restoration.

frontal face is in focus, whereas the frontal face of the other cube is out of focus, which is typical for digitally-reconstructed planes obtained from a hologram of a 3-D scene. Fig. 5c and d show the rescaled best-in-focus reconstructed planes obtained from the

hologram of the 3-D scene hidden behind a stationary diffuser. As seen from the latter figures, none of the patterns on the cubes can be recognized in any of these best-in-focus reconstructed planes. Fig. 5e and f show the rescaled best-in-focus reconstructed planes obtained from the hologram of the 3-D scene hidden behind the rotated/vibrated diffuser. Fig. 5e and f present a significant improvement compared to Fig. 5c and d, respectively.

Further improvement of the reconstructed 3-D image is obtained by digitally detecting the best step-edge of each plane and using it to estimate the system impulse response. Since the best step-edge is expected to be on the image of the best-in-focus objects in each reconstructed plane rather than on the image of the out-of-focus objects, using the estimated impulse response is expected to improve the best-in-focus image even more than the out-of-focus image in each plane. Fig. 5g and h show the rescaled best-in-focus reconstructed planes after applying the digital blind-convolution restoration algorithm, using $\eta = 0.005$ in Eq. (10). As shown in these figures, in spite of the noisy line patterns (which might look differently for other types of diffuser movements, rather than rotation), originated from light reflections from the diffuser and the not-fully-isotropic statistical properties of the optical system, the hidden objects can be recognized well compared to Fig. 5c and d, and even compared to Fig. 5e and f.

4. Conclusions

We have presented and experimentally demonstrated a new method of computing holograms of 3-D scenes hidden behind a turbulent medium. The experimental results given in Section 3 have demonstrated the method by generating a hologram of sim-ple 3-D objects hidden behind a diffusive, weakly-absorbing medium. The speckle ensemble method together with the digital blind restoration algorithm have restored the 3-D image of the hidden patterns with significantly better resolution, although these patterns could not be resolved at all in the case of a stationary diffuser. We believe that in the future the proposed holographic method might be useful for many practical applications, including observing 3-D objects embedded in biological tissues, 3-D imaging underwater, as well as 3-D imaging through the atmosphere. In spite of the potential of the proposed method, facing more absorptive, fairly thick, or highly diffusive turbulent media, that might characterize part of the abovementioned applications, is still a challenge to be solved.

References

[1] J.C. Hebden, S.R. Arridge, D.T. Delpy, Phys. Med. Biol. 42 (1997) 825.
[2] T. Vo-Dinh (Ed.), Biomedical Photonics Handbook, CRC Press, Boca Raton, 2003 (Chapters 13 and 16).
[3] S. Lévêque, A.C. Boccara, M. Lebec, H. Saint-Jalmes, Opt. Lett. 24 (1999) 181.
[4] J. Li, G. Ku, L.-H.V. Wang, Appl. Opt. 41 (2002) 6030.
[5] J. Rosen, D. Abookasis, Opt. Lett. 29 (2004) 253.
[6] D. Abookasis, J. Rosen, Opt. Lett. 31 (2006) 724.
[7] I. Moon, B. Javidi, Opt. Express 16 (2008) 13080.
[8] L. Yu, M.K. Kim, Opt. Lett. 30 (2005) 2092.
[9] O. Shacham, O. Haik, Y. Yitzhaky, Pattern Recogn. Lett. 28 (2007) 2094.
[10] N.T. Shaked, J. Rosen, Appl. Opt. 47 (2008) D21.
[11] J.W. Goodman, Introduction to Fourier Optics, second ed., McGraw-Hill, New York, 1996, p. 134.
[12] T. Vo-Dinh (Ed.), Biomedical Photonics Handbook, CRC Press, Boca Raton, 2003 (Chapter 21).
[13] J.F. Canny, IEEE Trans. Pattern Anal. Machine Intell. 8 (1986) 679.
[14] N.T. Shaked, J. Rosen, A. Stern, Opt. Express 15 (2007) 5754.
[15] N.T. Shaked, B. Katz, J. Rosen, Opt. Lett. 33 (2008) 1461.